Recent Methodological Enhancement of the ARIANE 5 SRBs Second Acoustic Mode Load Case

Samuel ROGEZ, Jean-François DURAND**, Benoît RYCKELYNCK*** and Frédéric BREVIERE*****
ASTRIUM Space Transportation
66, Route de Verneuil – 78133 Les Mureaux CEDEX – France
**samuel.rogez@astrium.eads.net*
***jean-francois.durand@astrium.eads.net*
****benoit.ryckelynck@astrium.eads.net*
*****frederic.breviere@astrium.eads.net*

Abstract

The acoustic Solid Rocket Booster (SRB) excitations of ARIANE 5 launcher are significant sources of responses that require accurate vibrations predictions.

Following a hardware evolution on the SRB, flight records are analyzed, focusing on the second acoustic booster mode. Based on flight observation, the precise phenomenology leading to the vibration blasts observed in flight is detailed. The central role of the damping requires introducing structural damping matrices to be fully representative of the in-flight coupling conditions.

The simulations performed using this methodology proves to be close to the flight measurement: it is a major improvement of the representativeness of the computation.

1. Introduction

During the second half of the Solid Rocket Boosters (SRB) flight phase, pressure oscillations appear in the boosters, due to acoustic modes excited by vortex sheddings in the combustion channel of the SRBs. As the boosters of ARIANE 5 provide 90% of the launcher thrust, these pressure oscillations can be particularly critical for the mechanical environment of the launcher and the payloads.
In order to reduce the launcher production cost, the bolted connections between the segments of the SRB were replaced by welded ones. Preliminary studies demonstrated a significant evolution in the dynamic behaviour of the SRB, with a potential impact on the vibration levels on the launcher. The second acoustic mode load case appeared to be the most sensitive as regards this hardware evolution.
This justified an accurate analysis of the flight records through a dedicated set of transducers and gave an opportunity to implement new features in the SRB second acoustic mode load case modelling.
This work has been performed thanks to ESA financial support.

2. Second acoustic booster mode phenomenon in flight

This section presents the post-flight analysis performed after the first flight with SRBs equipped with welded connections between the main segments.

The second acoustic mode load case on the ARIANE 5 launcher is the consequence of several interactions which take place between the excitation, the dynamic behaviour of the SRBs and the central body.
Inside the SRB, the excitation blasts are driven by the coupling between parietal vortices, internal protuberances and the acoustic modes of the cavity of the booster. The level of acceleration response on the booster depends on the excitation level and on the frequency gap between the excitation blasts and the booster modes.
For the central body of the launcher, the level of interaction is more complex: both SRBs have an influence on the dynamic behaviour of the central body, which is also characterised by its own modes. The following sections analyse these phenomena during ARIANE 5 L534 - V174 flight, equipped with welded connections on the SRBs.

2.1 Excitation inside the solid rocket booster

The internal dynamic pressure of the SRB is measured in flight with a sensor located in the vicinity of the booster igniter. The evolution of the power spectral density of this measurement during the flight is presented in Figure 1. Six blasts are clearly identified, as illustrated by the dark lines: they correspond to a coupling between the vortex shedding frequencies (characterized by several Strouhal lines) and the second acoustic mode of the cavity.
Maximum pressure values are reached during the first blast (b1). The maximal pressure decreases during the flight, from the first blast to the fourth one.

No major evolution is noticed concerning the pressure excitation in the SRB: the time and frequency at which the blasts occur, but also the level of excitation are similar to what is observed for SRBs with bolted connections. As a result, the change of the design of the connections has no impact on the pressure excitation.

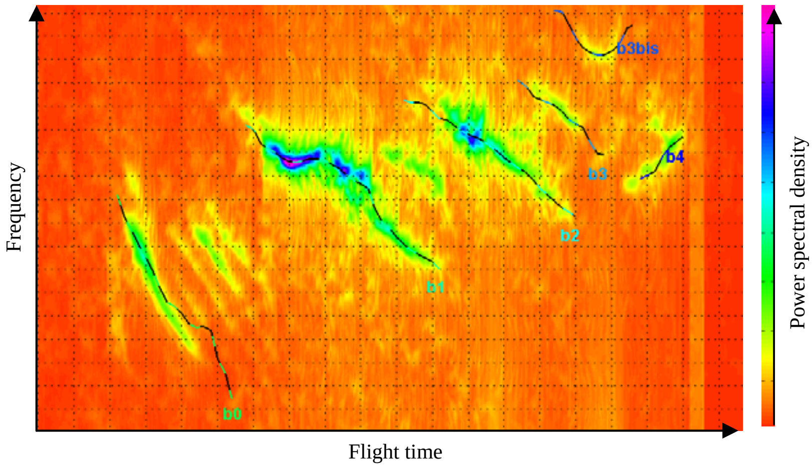

Figure 1: In-flight evolution of SRB internal pressure power spectral density

2.2 Mechanical mode of the booster

The first longitudinal mode is the main contributor to the SRB longitudinal response. In order to identify the SRB longitudinal mode, we calculate the ratio of the power spectral density of the SRB longitudinal acceleration response over the power spectral density of the excitation (SRB internal pressure). The SRB acceleration measurement used here is given by a sensor located in the upper part of the SRB: this part has a significant deformation which ensures good representativeness. The result is presented in Figure 2, where the longitudinal mode is highlighted by a black line (L-EAP1).

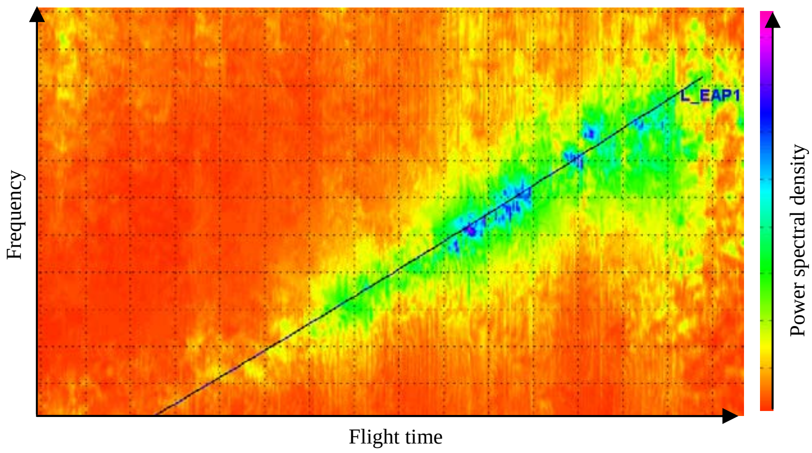

Figure 2: In-flight evolution of the SRB first longitudinal mode

The longitudinal acceleration response on the SRB depends on the frequency gap between the SRB longitudinal mode and the excitation blasts. This is highlighted in the figure 3, where the power spectral density of the longitudinal acceleration response of the SRB is presented, together with the excitation blasts and the SRB longitudinal mode evolutions identified above.

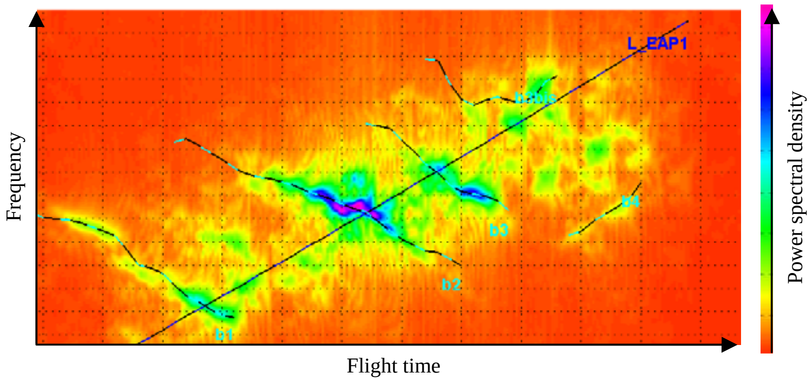

Figure 3: Longitudinal acceleration response of the SRB

The first blast yields low levels of response as the maximum excitation frequency is much higher than the longitudinal mode one. Yet, significant levels of forced response are reached at high frequency, which correspond to the maximum excitation levels.
During the second blast, the SRB longitudinal mode crosses the excitation blast when the excitation level is significant. This entails high level of longitudinal acceleration response on the SRBs.
The third blast excitation level is lower than the second one; however, as the longitudinal mode crosses the blast when its modal excitability is high, the acceleration responses are substantial.
Even if the excitation level is low for the blast identified as “b3 bis”, the longitudinal mode and the excitation frequencies are very close to each other: this leads to high levels of longitudinal response.
The excitation during the fourth blast is not negligible, but as the longitudinal mode is much higher in frequency, the resulting response is low as compared to the second and third blast ones.

One major impact of the connection design change on the SRB is a frequency shift of the SRB longitudinal mode. For welded connections, the mean SRB longitudinal mode frequency is slightly higher than for bolted connections. This point had been anticipated by predictions and was confirmed by post-flight analyses. An illustration is presented in figure 4, were several longitudinal frequencies are plot: they correspond to four flights for which welded connections were used on the SRBs (in green), and nine flights with bolted connections (in blue). No significant change is noticed regarding the corresponding excitation blasts evolutions, which are also presented for completeness.

As the main longitudinal mode frequency tends to be higher for SRBs with welded connections, it gets closer to the maximum excitation during the second blast. As a result, longitudinal responses are higher with welded connections during this blast. A similar phenomenon occurs during blast “b3 bis”: consequently, the acceleration levels are higher for SRBs with welded connections.

During the fourth blast, for SRB with welded connections, the longitudinal mode moves away from the excitation. This results in lower acceleration responses during this blast.

If the acceleration responses on the SRBs can be deduced from the interaction between the level of excitation and the coupling between the acoustic blast and the booster longitudinal mode, the analysis of the response of the central body of the launcher is more complex: it is presented in the following section.

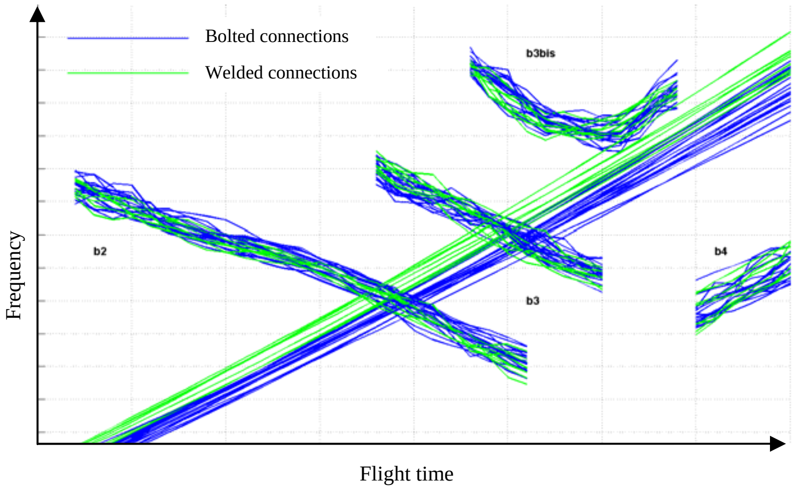

Figure 4: Evolution of SRB longitudinal mode from bolted to welded connections

2.3 Launcher central body behaviour

The conjunction of several phenomena contributes to the acceleration responses on the central body of the launcher:

- a set of three parameters for the first SRB; namely the level of excitation, the excitation frequency and the frequency of the SRB longitudinal mode,
- a similar set of parameters for the second SRB,
- the frequencies of the central body modes coupled with the SRBs.
- the complex time-combination of the excitations of both SRBs

This level of interaction is illustrated in figure 5, where a central body mode involving the main cryogenic stage oxygen tank lower bulkhead is plotted (FC), with the SRBs longitudinal modes (L_EAP1 and L_EAP2) and the excitation blasts. The response on this point is clearly driven by the coupling between these phenomena: maximum acceleration responses on this point are reached during the second and third blast, when the tank mode crosses the excitation blasts. As this crossing occurs in the vicinity of the SRBs longitudinal modes, the excitation transmitted to the central body is amplified by SRBs elongations.

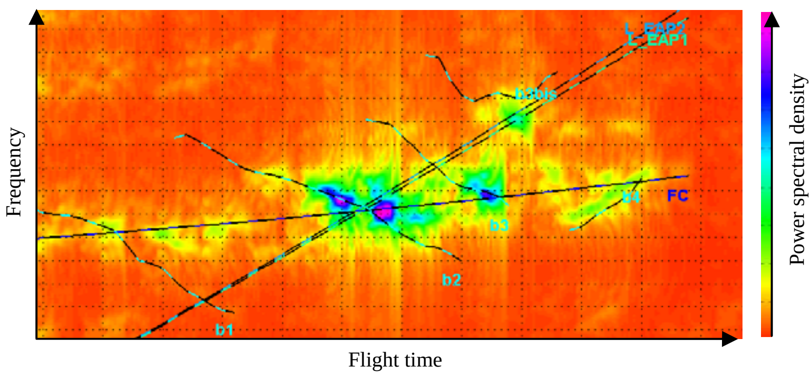

Figure 5: Longitudinal acceleration response at main cryogenic stage oxygen tank lower bulkhead

2.4 Conclusion

The analysis of the second acoustic booster mode in flight has shown that the level of response on both SRBs and on the central body of the launcher is highly dependent on the frequency of the longitudinal mode of the SRB. The post-flight analysis has shown a high level of interaction between the different parts of the launcher.

Several dynamic models are required in order to be fully representative of the complex couplings occurring due to the evolution of the SRB longitudinal mode frequency during the flight. They correspond to different flight times. Another key feature to model such complex couplings is the damping management, which is presented in the following section.

3. Damping management

3.1 Importance of off-diagonal terms of the damping matrix

The longitudinal mode of the SRB has been identified as the major contributor to the acceleration responses due to the second acoustic booster mode on the SRB and the central part of the launcher. This SRB longitudinal mode is characterised by a high damping value, as compared to the level of damping associated with central body modes.

As the excitation is applied to a structure whose damping is much different from other sub-structures ones, the classical assumption leading to a diagonal damping matrix is not satisfactory to model the couplings which occur in flight. Indeed, for this load-case, off-diagonal terms of the damping matrix have a first-order influence on the responses: this phenomenon is known as the coupling-through-damping effect.

This effect has been taken into account in the current simulation methodology, where structural damping matrices are used, in order to:

- define specific damping values for the different sub-structures of the launcher,
- build a fully populated damping matrix, which is representative of the couplings illustrated in post-flight analyses.

The damping management technique used is presented in the following section.

3.2 Damping matrices of the SRB

An excitability criterion is used to identify the SRB longitudinal mode in a Craig & Bampton condensed model of the booster. A specific viscous damping value is assigned to this longitudinal mode. This viscous damping value has been confirmed by a time-history simulation which is well correlated to the flight measurement (see figure 6).

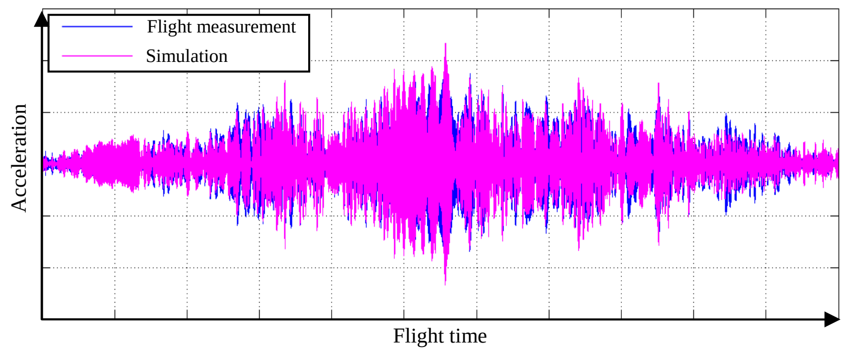

Figure 6: Validation of viscous damping value corresponding to the SRB longitudinal mode

A viscous damping matrix is considered for each SRB Craig & Bampton model. The matrix is divided into two parts as shown below.

$$\left[\underline{\Gamma}_{SRB}\right] = \begin{bmatrix} \underline{\Gamma}_{SRB}^{i} & 0 \\ 0 & \dfrac{\eta^{f}}{\omega}\overline{\underline{K}}_{SRB}^{\Sigma} \end{bmatrix} \quad \textbf{(1)}$$

The first part of the matrix $\underline{\Gamma}_{SRB}^{i}$ is a diagonal matrix corresponding to the SRB internal modes, defined as follows:

$$\left[\underline{\Gamma}_{SRB}^{i}\right] = \begin{bmatrix} \ddots & & & & & & \\ & 2\xi_{SRB}^{f}\omega_{SRB}\mu_{SRB} & & & & & \\ & & \ddots & & & & \\ & & & 2\xi_{SRB}^{longi}\omega_{SRB}\mu_{SRB} & & & \\ & & & & \ddots & & \\ & & & & & 2\xi_{SRB}^{f}\omega_{SRB}\mu_{SRB} & \\ & & & & & & \ddots \end{bmatrix} \quad \textbf{(2)}$$

where ω_{SRB} is the eigenfrequency of an internal mode of the SRB and μ_{SRB} is the corresponding generalized mass. The damping value is fixed at ξ_{SRB}^{f} for all internal modes except the longitudinal mode for which a specific value is used ξ_{SRB}^{longi}, as defined above.

The second part of the matrix $\dfrac{\eta^{f}}{\omega}\overline{\underline{K}}_{SRB}^{\Sigma}$ is the viscous damping equivalent to the hysteretic damping η^{f} for the interface degree of freedom of the SRB. ω is the pulsation of the SRB longitudinal mode.

The overall viscous damping matrix is associated with the internal modes of the SRBs. It is calculated as follows, using the eigenvector matrix $\left[\underline{\Phi}_{i}\right]_{SRB}$ containing the restriction of the launcher modal shapes on the internal modes of the SRBs:

$$\left[\underline{\Gamma}\right] = \sum_{SRB1,SRB2}\left[\underline{\Phi}_{i}\right]_{SRB}^{T}\left[\underline{\Gamma}_{SRB}^{i}\right]\left[\underline{\Phi}_{i}\right]_{SRB} \quad \textbf{(3)}$$

The top-level modal viscous damping matrix $\left[\underline{\Gamma}\right]$ is not diagonal: it includes coupling factors between the SRB modes and the launcher modes, what is well-representative of the real phenomenon in flight.

3.3 Damping of other sub-structures

Structural damping matrices are considered for other substructures. The structural damping matrix is calculated as:

$$\left[\underline{\Delta}\right] = \sum_{SS\in CB}\eta_{SS}\left[\underline{\Phi}_{SS}\right]^{T}\left[\underline{K}_{SS}\right]\left[\underline{\Phi}_{SS}\right] \quad \textbf{(4)}$$

where, for a given sub-structure (designated as "SS") of the central body, η_{SS} is the structural damping coefficient, $\left[\underline{\Phi}_{SS}\right]$ being the eigenvector matrix and $\left[\underline{K}_{SS}\right]$ the stiffness matrix.

For practical reasons, the equivalent viscous damping of the interface degrees of freedom of the SRB is integrated into the structural damping matrix:

$$\left[\underline{\Delta}\right] = \sum_{SS\in CB}\eta_{SS}\left[\underline{\Phi}_{SS}\right]^{T}\left[\underline{K}_{SS}\right]\left[\underline{\Phi}_{SS}\right] + \sum_{SRB1,\,SRB2}\eta^{f}\left[\underline{\Phi}_{SRB}^{\Sigma}\right]^{T}\overline{\underline{K}}_{SRB}^{\Sigma}\left[\underline{\Phi}_{SRB}^{\Sigma}\right] \quad \textbf{(5)}$$

This method enables to define different structural damping coefficients for different sub-structures, based on the results of modal survey tests.

3.4 Resolution

Once the modal viscous damping matrix $[\underline{\Gamma}]$ and the modal structural damping matrix $[\underline{\Delta}]$ have been defined, the acceleration responses $\underline{\ddot{u}}(\omega)$ are calculated:

$$\underline{\ddot{u}}(\omega) = -\omega^2 [\underline{\Phi}]\left(-\omega^2 \lfloor \underline{\mu} \rfloor + j\omega[\underline{\Gamma}] + [\underline{\Lambda}] + j[\underline{\Delta}]\right)^{-1} [\underline{\Phi}]^T \underline{f}(\omega) \tag{6}$$

where:

- ω is the frequency at which the response is calculated,
- $[\underline{\Phi}]$ is the launcher eigenvector matrix,
- $\lfloor \underline{\mu} \rfloor$ and $[\underline{\Lambda}]$ are the launcher generalized mass and stiffness matrices,
- $\underline{f}(\omega)$ is the external forces vector.

4. Comparison to flight measurement

Simulations are performed using the method presented in the previous section: the results are compared to the flight measurements.

The excitation in each booster is tuned in order to recover the level of longitudinal acceleration measured in flight on the SRB. Both SRBs are loaded and their influences on the central body of the launcher are added: this corresponds to the worst-case scenario in terms of combination, as a phase shift may exist between the two loadings, resulting in a potentially lower cumulated loading on the central body of the launcher.

The SRB damping matrices are built in conformity with the method described above. Specific structural damping coefficients are used for the tanks of the main cryogenic stage, for both tanks of the upper stage and for the payloads.

Three simulations have been performed to take into account the evolution of the SRB model during the flight. The results are compared to the flight measurements. The acceleration responses of several sensors distributed on the launcher are presented in figure 7. Six shock response spectra have been calculated from flight measurement at the flight times corresponding to the simulations.

The flight measurements presented in figure 7 have significant magnitude, as compared to the level of quantification of each sensor.

Simulation and flight measurement show good correlation. Simulation results on SRBs (sensors n°1 and 3) are well representative of the booster dynamic behaviour in flight conditions. The central body responses are accurate as far as the frequency position of the main peak is concerned (sensor 2, 4, 5 and 6). The acceleration responses levels on the central body are close to flight measurements.

Finally, the method gives satisfactory results as compared to flight measurements.

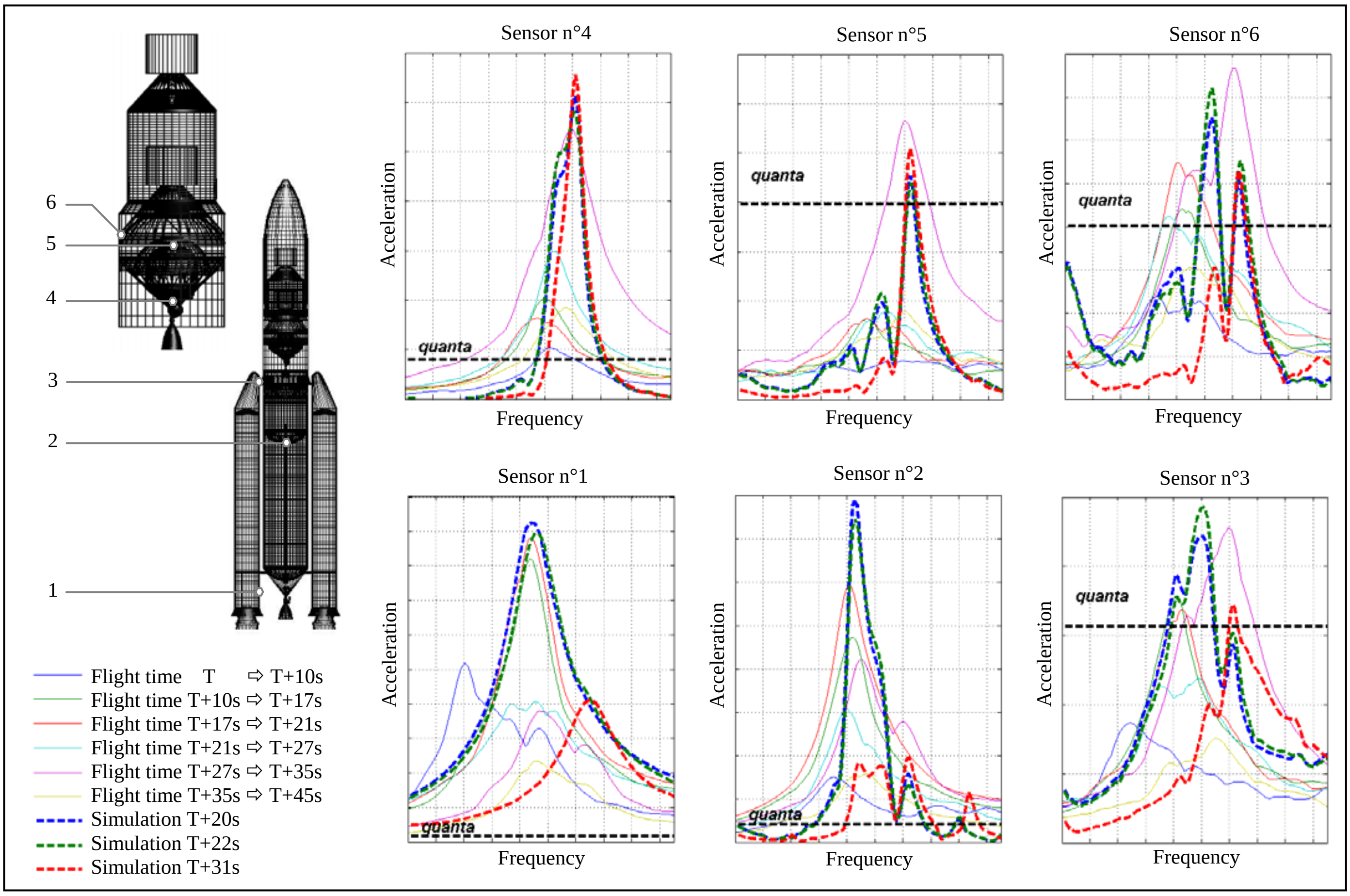

Figure 7: Comparison between simulation results and flight measurements

5. Conclusion

A raise of the vibration responses due to the second acoustic booster mode load case was foreseen as the consequence of the modification of the main segments interfaces of ARIANE 5 SRBs (from bolted to welded connections).

The first flight equipped with the new hardware is deeply analyzed: the precise phenomenology leading to the vibration blasts observed in flight is detailed. The complex coupling effects between the acoustic excitation in the booster cavity, the mechanical mode of the SRB and the launcher longitudinal modes are highlighted. Several simulations have to be performed to take into account the evolution of the SRB longitudinal mode in flight. The evidence of the central role of the damping in the couplings requires reviewing the damping methodology.

Introducing structural damping matrices enables to be representative of the physical phenomena and especially the coupling-through-damping effect. SRB damping matrices are elaborated using a Craig-Bampton condensation scheme: a dedicated damping value is assigned to the main SRBs modes. Structural damping matrices are defined for the different sub-components of the central body of the launcher, leading to a full damping matrix for the complete assembled launcher model.

The simulations performed using this methodology are well correlated with the flight measurement. The damping modelling process enhancement ensures a complete mathematic consistency. It is a major achievement for the reliability of the computation process.

The use of such an approach can be contemplated for other load cases for which off-diagonal terms of the damping matrix have significant influence.